Tunable two-axis spin model and spin squeezing in two cavities*

Lixian Yu(俞立先)[1], Caifeng Li(李彩凤)[2,3], Jingtao Fan(樊景涛)[2], Gang Chen(陈刚)[2,5,†], Tian-Cai Zhang(张天才)[4,5], and Suotang Jia(贾锁堂)[2,5]

[1] *Department of Physics, Shaoxing University, Shaoxing* 312000, *China*
[2] *State Key Laboratory of Quantum Optics and Quantum Optics Devices, Institute of Laser spectroscopy, Shanxi University, Taiyuan* 030006, *China*
[3] *Institute of Theoretical Physics, Shanxi University, Taiyuan* 030006, *China*
[4] *State Key Laboratory of Quantum Optics and Quantum Optics Devices, Institute of Opto-Electronics, Shanxi University, Taiyuan* 030006, *China*
[5] *Collaborative Innovation Center of Extreme Optics, Shanxi University, Taiyuan* 030006, *China*

(Received 14 November 2015; revised manuscript received 6 January 2016; published online 5 April 2016)

Multi-mode cavities have now attracted much attention both experimentally and theoretically. In this paper, inspired by recent experiments of cavity-assisted Raman transitions, we realize a two-axis spin Hamiltonian $H = q(J_x^2 + \chi J_y^2) + \omega_0 J_z$ in two cavities. This realized Hamiltonian has a distinct property that all parameters can be tuned independently. For proper parameters, the well-studied one- and two-axis twisting Hamiltonians are recovered, and the scaling of N^{-1} of the maximal squeezing factor can occur naturally. On the other hand, in the two-axis twisting Hamiltonian, spin squeezing is usually reduced when increasing the atomic resonant frequency ω_0. Surprisingly, we find that by combining with the dimensionless parameter $\chi(>-1)$, this atomic resonant frequency ω_0 can enhance spin squeezing greatly. These results are beneficial for achieving the required spin squeezing in experiments.

Keywords: two-axis spin model, spin squeezing, two cavities

PACS: 03.65.Vf, 42.50.Ct, 42.50.Pq **DOI:** 10.1088/1674-1056/25/5/050301

1. Introduction

Squeezed spin states, which were first introduced by Kitagawa and Ueda,[1] are quantum correlated states with reduced fluctuations in one of the collective spin components.[2,3] Such states have attracted considerable interest because they not only play significant roles in investigating many-body entanglement,[4,5] but also have important applications in atom interferometers and high-precision atom clocks.[6,7] In general, there are two methods to produce spin squeezing. One is based on a one-axis twisting Hamiltonian $H_{\rm OAT} = qJ_x^2$, where q is the nonlinear spin–spin interaction strength and J_x is the collective spin operator in the x direction. When the initial state is prepared as $|J_z = -j\rangle$ for $q > 0$ ($|J_z = j\rangle$ for $q < 0$), the maximal squeezing factor for this one-axis twisting Hamiltonian scales as $N^{-2/3}$,[1] where N is the total atomic number and $J = N/2$. In contrast, for the other two-axis twisting Hamiltonian $H_{\rm TAT} = q(J_x^2 - J_y^2)$, the maximal squeezing factor scales as N^{-1} with the same initial state.[1] Since the scaling of N^{-1} approaches the Heisenberg limit, implementing the two-axis twisting Hamiltonian in current experimental setups is very important and necessary.[8–15] A possible scheme is to transform the one-axis twisting Hamiltonian into the two-axis twisting Hamiltonian by applying pulse sequences or continuous driving in the two-component Bose–Einstein condensates.[16–19] However, the experimental achievement of such two-axis twisting Hamiltonian is still challenging.

The ultrahigh-finesse cavities interacting with two-level particles (such as atoms, nitrogen vacancy centers, superconducting qubits, etc) are also powerful platforms to produce effective spin squeezing, since the photon of cavity mode can induce nonlinear spin–spin interaction and thus generate the required one-axis twisting Hamiltonian.[20–30] Recently, multi-mode cavities[31] have attracted much attention both experimentally and theoretically.[32–37] On one hand, these setups can be used to explore novel physics, such as the spin-orbit-induced anomalous Hall effect,[38,39] the crystallization and frustration,[40,41] the spin glass,[42–45] and the gapless Nambu–Goldstone-type mode without rotating-wave approximation.[46] Moreover, two-mode field squeezing[47] and unconditional preparation of a two-mode squeezed state of effective bosonic modes[48] have also been achieved by introducing two cavities.

In this paper, inspired by recent experiments of cavity-assisted Raman transitions,[49,50] we mainly realize a generalized two-axis spin Hamiltonian $H = q(J_x^2 + \chi J_y^2) + \omega_0 J_z$, where χ is an anisotropic parameter and ω_0 is an effective atomic resonant frequency, when an ensemble of ultracold six-level atoms interacts with two quantized cavity fields and two pairs of Raman lasers. The Hamiltonian achieved has a distinct property that the interaction strength q, the anisotropic

*Project supported by the National Natural Science Foundation of China (Grant Nos. 11422433, 11447028, 61227902, 11434007, and 61275211), the Natural Science Foundation of Zhejiang Province, China (Grant No. LY13A040001), and the Scientific Research Foundation of the Education Department of Zhejiang Province, China (Grant No. Y201122352).

†Corresponding author. E-mail: chengang971@163.com

© 2016 Chinese Physical Society and IOP Publishing Ltd

parameter χ, and the effective atomic resonant frequency ω_0 can be tuned independently. For reasonable parameters, the well-studied one- and two-axis twisting Hamiltonians are recovered. Numerical results reveal that for the standard two-axis twisting Hamiltonian ($\chi = -1$ and $\omega_0 = 0$), the corresponding maximal squeezing factor scales as N^{-1}, as expected. On the other hand, in the two-axis twisting Hamiltonian $H_{\rm TAT}$, spin squeezing is usually reduced when increasing the effective atomic resonant frequency ω_0Surprisingly, we find that by combining with the anisotropic parameter χ (> -1), this effective atomic resonant frequency ω_0 can enhance spin squeezing greatly. These results are of benefit for achieving the required spin squeezing in experiments.

2. Two-axis spin Hamiltonian with independently-tunable parameters

Figure 1(a) shows our proposal, in which an ensemble of ultracold six-level atoms interacts with two quantized cavity fields and two pairs of Raman lasers. These six levels consist of two stable ground states ($|0\rangle$ and $|1\rangle$) and four excited states ($|r_1\rangle$, $|r_1\rangle$, $|s_1\rangle$, and $|s_2\rangle$) (see Fig. 1(b)). For ^{87}Rb atom, the detailed levels can be chosen as $|0\rangle \to 5S_{1/2}\,|F=1,m_F=0\rangle$, $|1\rangle \to 5S_{1/2}\,|F=2,m_F=0\rangle$, $|r_1\rangle \to 5P_{1/2}\,|F=1,m_F=0\rangle$, $|s_1\rangle \to 5P_{3/2}\,|F=1,m_F=0\rangle$, $|r_2\rangle \to 5P_{1/2}\,|F=1,m_F=-1\rangle$, and $|s_2\rangle \to 5P_{3/2}\,|F=1,m_F=-1\rangle$. Two independent photon modes, whose creation and annihilation operators are $a^\dagger$ ($b^\dagger$) and a (b), mediate the $|0\rangle \longleftrightarrow |s_1\rangle$ and $|1\rangle \longleftrightarrow |r_1\rangle$ ($|0\rangle \longleftrightarrow |s_2\rangle$ and $|1\rangle \longleftrightarrow |r_2\rangle$) transitions (red and blue solid lines) with atom–photon coupling strengths g_{s_1} (g_{s_2}) and g_{r_1} (g_{r_2}), respectively. Whereas two pairs of Raman lasers govern the other transitions $\{|0\rangle \longleftrightarrow |r_1\rangle, |1\rangle \leftrightarrow |s_1\rangle\}$ and $\{|0\rangle \longleftrightarrow |r_2\rangle, |1\rangle \longleftrightarrow |s_2\rangle\}$ (red and blue dashed lines) with Rabi frequencies $\{\Omega_{r_1}, \Omega_{s_1}\}$ and $\{\Omega_{r2}, \Omega_{s_2}\}$, respectively. $\Delta_{r_{1,2}}$ and $\Delta_{s_{1,2}}$ are the detunings from the excited states.

The total Hamiltonian illustrated in Fig. 1 can be written, under the rotating wave approximation, as

$$H_{\rm T} = H_{\rm C} + H_{\rm A} + H_{\rm I}, \tag{1}$$

where

$$\begin{aligned} H_{\rm C} &= \omega_{\rm a} a^\dagger a + \omega_{\rm b} b^\dagger b, \qquad (2)\\ H_{\rm A} &= \sum_{j=1}^{N} \{\omega_{r_1} |r_1\rangle_j \langle r_1|_j + \omega_{r_2} |r_2\rangle_j \langle r_2|_j + \omega_{s_1} |s_1\rangle_j \langle s_1|_j \\ &\quad + \omega_{s_2} |s_2\rangle_j \langle s_2|_j + \omega_1 |1\rangle_j \langle 1|_j \\ &\quad + \frac{1}{2}\big[\Omega_{s_1} |s_1\rangle_j \langle 1|_j \, {\rm e}^{-{\rm i}(\omega_{1s_1} t - \varphi_{s_1})} \\ &\quad + \Omega_{s_2} |s_2\rangle_j \langle 1|_j \, {\rm e}^{-{\rm i}(\omega_{1s_2} t - \varphi_{s_2})} \\ &\quad + \Omega_{r_1} |r_1\rangle_j \langle 0|_j \, {\rm e}^{-{\rm i}(\omega_{0r_1} t - \varphi_{r_1})} \\ &\quad + \Omega_{r_2} |r_2\rangle_j \langle 0|_j \, {\rm e}^{-{\rm i}(\omega_{0r_2} t - \varphi_{r_2})} + {\rm H.c.}\big]\}, \qquad (3) \end{aligned}$$

$$\begin{aligned} H_{\rm I} &= \sum_{j=1}^{N} \big[g_{s_1} |s_1\rangle_j \langle 0|_j a + g_{r_1} |r_1\rangle_j \langle 1|_j a \\ &\quad + g_{s_2} |s_2\rangle_j \langle 0|_j b + g_{r_2} |r_2\rangle_j \langle 1|_j b + {\rm H.c.}\big]. \qquad (4) \end{aligned}$$

In the Hamiltonians (2)–(4), $\omega_{r_{1,2}}$, $\omega_{s_{1,2}}$, and ω_1 are the atomic frequencies, $\omega_{1s_{1,2}}$ ($\varphi_{s_{1,2}}$) and $\omega_{0r_{1,2}}$ ($\varphi_{r_{1,2}}$) are the frequencies (phases) of Raman lasers, respectively, and H.c. denotes the Hermitian conjugate.

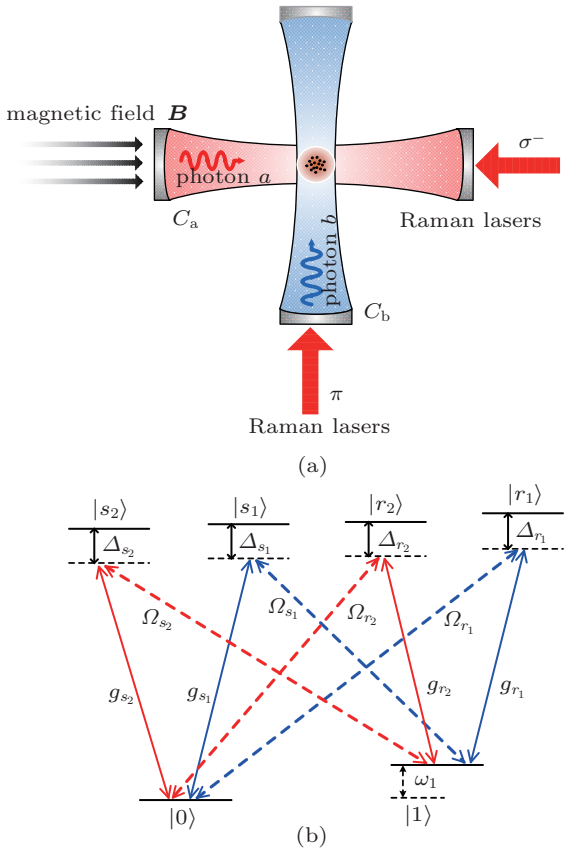


Fig. 1. (color online) (a) Proposed experimentally-feasible setup that an ensemble of ultracold six-level atoms interacts with two quantized cavity fields and two pairs of Raman lasers. A couple of orthogonally placed cavities $C_{\rm a}$ and $C_{\rm b}$ are arranged in a specific plane, and a guided magnetic field $\boldsymbol{B}$ is applied along one of the two cavities (see, for example, $C_{\rm a}$) to fix a quantized axis and split the Zeeman sublevels of the atomic ensemble. Both the cavity modes and Raman lasers propagated in $C_{\rm a}$ ($C_{\rm b}$) are assumed to be right-handed circularly polarized (linearly polarized along the guided magnetic field $\boldsymbol{B}$). (b) Energy-level structure and their transitions induced by two photon modes and two pairs of Raman lasers. For ^{87}Rb atom, the detailed levels can be chosen as $|0\rangle \to 5S_{1/2}\,|F=1,m_F=0\rangle$, $|1\rangle \to 5S_{1/2}\,|F=2,m_F=0\rangle$, $|r_1\rangle \to 5P_{1/2}\,|F=1,m_F=0\rangle$, $|s_1\rangle \to 5P_{3/2}\,|F=1,m_F=0\rangle$, $|r_2\rangle \to 5P_{1/2}\,|F=1,m_F=-1\rangle$, and $|s_2\rangle \to 5P_{3/2}\,|F=1,m_F=-1\rangle$. In such an arrangement, the transitions labeled by the red lines (blue lines) are thus π transitions (σ^- transitions).

By means of the Hamiltonian (1), we first realize a two-mode Dicke model with independently-tunable parameters. In the interaction picture with respect to the free Hamiltonian

$$\begin{aligned} H_0 &= \widetilde{\omega_{\rm a}} a^\dagger a + \widetilde{\omega_{\rm b}} b^\dagger b \\ &\quad + \sum_{j=1}^{N} \big(\widetilde{\omega_{s_1}} |s_1\rangle_j \langle s_1|_j + \widetilde{\omega_{r_1}} |r_1\rangle_j \langle r_1|_j \\ &\quad + \widetilde{\omega_{s_2}} |s_2\rangle_j \langle s_2|_j + \widetilde{\omega_{r_2}} |r_2\rangle_j \langle r_2|_j + \widetilde{\omega_1} |1\rangle_j \langle 1|_j\big), \end{aligned}$$

where $\widetilde{\omega_{\rm a}} = \widetilde{\omega_{s_1}} = (\omega_{0r_1} + \omega_{1s_1})/2$, $\widetilde{\omega_{\rm b}} = \widetilde{\omega_{s_2}} = (\omega_{0r_2} + \omega_{1s_2})/2$, $\widetilde{\omega_1} = (\omega_{0r_1} - \omega_{1s_1})/2 = (\omega_{0r_2} - \omega_{1s_2})/2$, $\widetilde{\omega_{r_1}} = \widetilde{\omega_1} + \widetilde{\omega_{\rm a}}$, and $\widetilde{\omega_{r_2}} = \widetilde{\omega_1} + \widetilde{\omega_{\rm b}}$, the Hamiltonian (1) can be rewritten as (see Appendix A)

$$\begin{aligned}\widetilde{H} &= \omega_{\rm A} a^\dagger a + \omega_{\rm B} b^\dagger b + \omega_0 J_z \\ &\quad + \lambda_1 J_x (a^\dagger + a) + \lambda_2 J_y (b^\dagger + b). \end{aligned} \tag{5}$$

Here $J_x = (J_+ + J_-)/2$ and $J_y = -{\rm i}(J_+ - J_-)/2$, with $J_+ = \sum_{j=1}^{j=N} |1\rangle_j \langle 0|_j$, $J_- = \sum_{j=1}^{j=N} |0\rangle_j \langle 1|_j$, and $J_z = \sum_{j=1}^{j=N} (|1\rangle_j \langle 1|_j - |0\rangle_j \langle 0|_j)/2$, are the collective spin operators, and $\omega_{\rm A} = \Delta_{\rm a} + \frac{1}{2}\left(N g_{r_1}^2/\Delta_{r1} + N g_{s_1}^2/\Delta_{s1}\right)$, $\omega_{\rm B} = \Delta_{\rm b} + \frac{1}{2}\left(N g_{r_2}^2/\Delta_{r_2} + N g_{s_2}^2/\Delta_{s_2}\right)$ are the effective cavity frequencies, $\omega_0 = \Delta_1 + \frac{1}{4}\left(\Omega_{s_1}^2/\Delta_{s_1} + \Omega_{s_2}^2/\Delta_{s_2} - \Omega_{r_1}^2/\Delta_{r_1} - \Omega_{r_2}^2/\Delta_{r_2}\right)$ is the effective resonant atomic frequency, $\lambda_1 = \Omega_{s_1} g_{s_1}/\Delta_{s_1} = \Omega_{r_1} g_{r_1}/\Delta_{r_1}$ and $\lambda_2 = \Omega_{s_2} g_{s_2}/\Delta_{s_2} = \Omega_{r_2} g_{r_2}/\Delta_{r_2}$ are the effective atom photon coupling strengths, with $\Delta_{\rm a} = \omega_{\rm a} - \widetilde{\omega_{\rm a}}$, $\Delta_{\rm b} = \omega_{\rm b} - \widetilde{\omega_{\rm b}}$, $\Delta_{s_1} = \omega_{s_1} - \widetilde{\omega_{s_1}}$, $\Delta_{s_2} = \omega_{s_2} - \widetilde{\omega_{s_2}}$, and $\Delta_1 = \omega_1 - \widetilde{\omega_1}$. We show that the Hamiltonian (5) is our realized two-mode Dicke model, based on recent experiments of cavity-assisted Raman transitions.[49,50] In contrast to the convectional two-mode Dicke model achieved in the two-level atoms, the Hamiltonian (5) has a distinct property that all parameters can be tuned independently. For example, $\omega_{\rm A}$ and $\omega_{\rm B}$ as we mentioned depend on the detunings $\Delta_{\rm a}$ and $\Delta_{\rm b}$, respectively. Thus, they can range from the positive to the negative. The choice of the different cavity frequencies $\omega_{\rm A}$ and $\omega_{\rm B}$ help us to create a tunable two-axis spin Hamiltonian, see below. The effective atomic resonant frequency ω_0 can also be controlled by the detuning Δ_1. In addition, the effective atom–photon coupling strengths λ_1 and λ_2 can be driven by the Rabi frequencies of Raman lasers, respectively.

We now introduce two new unitary transformations, $U_1 = \exp\left[G_1 J_x (a^\dagger - a)\right]$ and $U_2 = \exp\left[G_2 J_y (b^\dagger - b)\right]$ with $G_1 = \lambda_1/\omega_{\rm A}$ and $G_2 = \lambda_2/\omega_{\rm B}$, to rewrite the Hamiltonian (5) as

$$\begin{aligned} H &= U_2 U_1 \widetilde{H} U_1^\dagger U_2^\dagger \\ &= \omega_{\rm A}(a^\dagger - G_1 J_x)(a - G_1 J_x) + \omega_{\rm B}(b^\dagger - G_2 J_y)(b - G_2 J_y) \\ &\quad + \omega_0 \{[J_z \cosh[G_2(b^\dagger - b)] + {\rm i} J_x \sinh[G_2(b^\dagger - b)]] \\ &\quad \times \cosh[G_1(a^\dagger - a)] - {\rm i} J_z \sinh[G_2(b^\dagger - b)]\} \\ &\quad + \lambda_1 \{J_x \cosh[G_2(b^\dagger - b)] - {\rm i} J_z \sinh[G_2(b^\dagger - b)]\} \\ &\quad \times \{a^\dagger + a - 2G_1 [J_x \cosh[G_2(b^\dagger - b)] \\ &\quad - {\rm i} J_y \sinh[G_1(a^\dagger - a)]\} + \lambda_2 \{J_y \cosh[G_1(a^\dagger - a)] \\ &\quad + {\rm i}[J_z \cosh[G_2(b^\dagger - b)] + {\rm i} J_x \sinh[G_2(b^\dagger - b)]] \\ &\quad \times \sinh[G_1(a^\dagger - a)]\}(b^\dagger + b - 2G_2 J_y). \end{aligned}$$

In the dispersive regime ($\{|\omega_{\rm A}|, |\omega_{\rm B}|\} \gg \{\lambda_1, \lambda_2\}$), we can expand the Hamiltonian H with respect to G_1 and G_2 (up to second order). In addition, in such limit, the cavity modes only support the excitation of virtual photons ($\langle a^\dagger a \rangle \to 0$ and $\langle b^\dagger b \rangle \to 0$),[20–27] i.e., all terms with respect to the photons are eliminated. As a consequence, the Hamiltonian H turns into

$$H = q(J_x^2 + \chi J_y^2) + \omega_0 J_z, \tag{6}$$

where

$$q = -\frac{\lambda_1^2}{\omega_{\rm A}}, \tag{7}$$

$$\chi = \frac{\omega_{\rm A} \lambda_2^2}{\omega_{\rm B} \lambda_1^2}. \tag{8}$$

In the Hamiltonian (6), the parameter q determines the nonlinear spin–spin interaction J_x^2 induced by the virtual photon, and the anisotropic parameter χ reflects the ratio between the different nonlinear spin–spin interactions J_x^2 and J_y^2. Due to existence of these nonlinear spin–spin interactions with the anisotropic parameter χ and the effective atomic resonant frequency ω_0, here we call the Hamiltonian (6) a generalized two-axis spin Hamiltonian. In addition, It shows clearly that all the parameters, including the interaction strength q, the anisotropic parameter χ, and the effective atomic resonant frequency ω_0, can also be tuned independently in experiments.

For different parameters, the generalized two-axis spin Hamiltonian (6) can reduce to some well-studied Hamiltonians. For example, when $\chi > 0$, the Hamiltonian (6) becomes a standard Lipkin–Meshkov–Glick model.[52–58] When $\omega_0 = 0$, the Hamiltonian (6) reduces to a generalized two-axis twisting Hamiltonian $H_{\rm GTAT} = q(J_x^2 + \chi J_y^2)$. If further setting $\chi = -1$, a standard two-axis twisting Hamiltonian $H_{\rm TAT} = q(J_x^2 - J_y^2)$ is derived. Finally, when $\chi = 0$, the Hamiltonian (6) turns into a generalized one-axis twisting Hamiltonian $H_{\rm GOAT} = q J_x^2 + \omega_0 J_z$,[59–63] which reduces to the standard one-axis twisting Hamiltonian $H_{\rm OAT} = q J_x^2$ for $\omega_0 = 0$. These results imply that the Hamiltonian (6) has an important application in achieving the required spin squeezing.

Notice that when $\omega_{\rm A} < 0$, the effective spin–spin interaction strength $q > 0$. Thus, we can use the initial state $|J_z = -j\rangle$ to discuss spin squeezing of the generalized two-axis spin Hamiltonian (6). This initial state $|J_z = -j\rangle$ can be easily prepared in experiments.

3. Spin squeezing factor

In order to investigate spin squeezing, it is very necessary to consider the following time-dependent squeezing factor:[1]

$$\xi_{\rm S}^2(t) = \frac{4}{N} \min\left[\Delta J_{\boldsymbol{n}_\perp}^2(t)\right], \tag{9}$$

where $\boldsymbol{n}_\perp$ refers to an axis, which is perpendicular to the mean-spin direction $\boldsymbol{n}_0 = \boldsymbol{J}/|J|$ with $|J| = \sqrt{\langle J_x\rangle^2 + \langle J_y\rangle^2 + \langle J_z\rangle^2}$, and $\Delta A^2 = \langle A^2\rangle - \langle A\rangle^2$ is the standard deviation. If $\left|\xi_{\rm S}^2(t)\right| < 1$, the spin state is squeezed, and vice versa. It should be noticed that here we do not use another

spin squeezing factor $\xi_{\rm R}^2(t)$ proposed by Wineland *et al.*[64] in the study of Ramsey spectroscopy, which is substantially connected to the phase sensitivity in experiments. In fact, $\xi_{\rm R}^2(t)$ is related to $\xi_{\rm S}^2(t)$ via $\xi_{\rm R}^2(t) = (N/2|J|)^2\xi_{\rm S}^2(t)$.

In the spherical coordinates, $\boldsymbol{n}_0 = (\sin\theta\cos\varphi, \sin\theta\sin\varphi, \cos\theta)$, where $\theta = \arccos(\langle J_z\rangle/|J|)$, and $\varphi = \arccos(\langle J_x\rangle/|J|\sin\theta)$ for $\langle J_y\rangle > 0$ or $\varphi = 2\pi - \arccos(\langle J_x\rangle/|J|\sin\theta)$ for $\langle J_y\rangle \leq 0$. Two orthogonal bases are given by $\boldsymbol{n}_1 = (-\sin\varphi, \cos\varphi, 0)$ and $\boldsymbol{n}_2 = (-\cos\theta\cos\varphi, \cos\theta\sin\varphi, -\sin\theta)$. Thus, $J_{\boldsymbol{n}_{1,2}} = \boldsymbol{J}\cdot\boldsymbol{n}_{1,2}$, $J_{\boldsymbol{n}_\perp} = J_{\boldsymbol{n}_1}\cos\phi + J_{\boldsymbol{n}_2}\sin\phi$, and $\min(\Delta J_{\boldsymbol{n}_\perp}^2)$ could be achieved, when ϕ varies from 0 to 2π in the plane that is perpendicular to the mean-spin direction $\boldsymbol{n}_0$. It should be noticed that in experiments, the maximal squeezing factor

$$\xi_{\rm M}^2 = \min\left[\xi_{\rm S}^2(t)\right] \tag{10}$$

is usually measured.[2,3] Thus, in the following discussion, we mainly focus on this physical quantity.

Before proceeding, we check the validity of the Hamiltonian (6), when the initial state is chosen as $|J_z = -j\rangle$. For the generalized two-axis spin Hamiltonian, it is very hard to obtain the analytical result of the spin squeezing factor $\xi_{\rm S}^2(t)$.[2] In Fig. 2, we plot the corresponding spin squeezing factors $\xi_{\rm S}^2(t)$ of the Hamiltonians (5) and (6). It can be seen clearly that the results of the Hamiltonian (6) are almost identical to those of the Hamiltonian (5). Therefore, we will apply the Hamiltonian (6) to discuss the experimentally measurable maximal squeezing factor $\xi_{\rm M}^2$ in the rest of this paper.

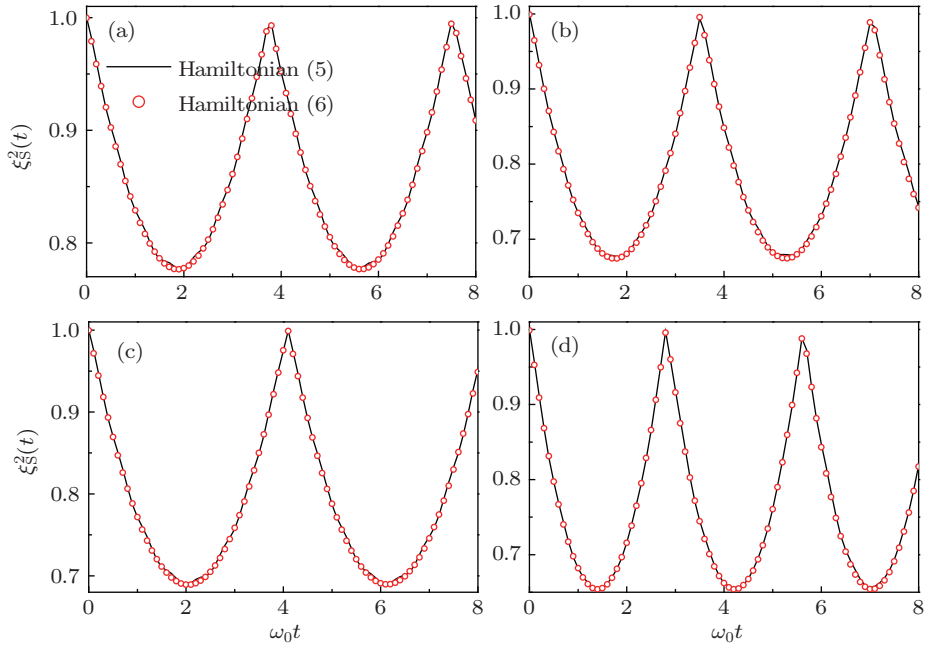


Fig. 2. (color online) Numerical plot of the time-dependent spin squeezing factors $\xi_{\rm S}^2(t)$ of both the Hamiltonians (5) and (6), with the same initial states $|J_z = -j\rangle$. In panels (a) and (b), $\omega_{\rm A}/\omega_0 = 200$, $\omega_{\rm B}/\omega_0 = \pm 200$ ["+" for (a) and "−" for (b)], $\lambda_1/\omega_0 = 2$, $\lambda_2/\omega_0 = 1$, and $N = 15$. In panels (c) and (d), $\omega_{\rm A}/\omega_0 = 200$, $\omega_{\rm B}/\omega_0 = \pm 200$ ["+" for (c) and "−" for (d)], $\lambda_1/\omega_0 = 1$, $\lambda_2/\omega_0 = 2$, and $N = 20$.

4. Maximal squeezing factor

We first address a simple case without the effective atomic resonant frequency ($\omega_0 = 0$), in which the generalized two-axis spin Hamiltonian (6) reduces to the generalized two-axis twisting Hamiltonian $H_{\rm GTAT} = q(J_x^2 + \chi J_y^2)$. In Fig. 3, we numerically plot the maximal squeezing factor $\xi_{\rm M}^2$ of the Hamiltonian $H_{\rm GTAT}$ as a function of the atomic number N for the different anisotropic parameters χ, when the initial state is chosen as $|J_z = -{\rm j}\rangle$. This figure shows clearly that when $\chi = 0$, the generalized two-axis twisting Hamiltonian $H_{\rm GTAT}$ becomes the standard one-axis twisting Hamiltonian $H_{\rm OAT} = qJ_x^2$, whose maximal squeezing factor $\xi_{\rm M}^2$ scales as $N^{-2/3}$.[1] When increasing the anisotropic parameter χ, the maximal squeezing factor $\xi_{\rm M}^2$ decreases, i.e., spin squeezing is enhanced. In particular, when $\chi = -1$, the Hamiltonian $H_{\rm GTAT}$ turns into the standard two-axis twisting Hamiltonian $H_{\rm TAT} = q(J_x^2 - J_y^2)$, whose maximal squeezing factor $\xi_{\rm M}^2$ scales as N^{-1},[1] as expected. In addition, the maximal squeezing factor $\xi_{\rm M}^2$ as a function of the anisotropic parameter χ is also plotted in the insert part of Fig. 3. This figure shows that $\chi = -1$ is an optimal point to achieve the maximal squeezing factor $\xi_{\rm M}^2$ of the generalized two-axis twisting Hamiltonian $H_{\rm GTAT}$.

In the real experiments, the effective atomic resonant frequency ω_0 always exists. In Fig. 4, we numerically plot the maximal squeezing factor $\xi_{\rm M}^2$ of the Hamiltonian $H = q(J_x^2 - J_y^2) + \omega_0 J_z$ as a function of the effective atomic resonant frequency ω_0, when the the initial state is chosen as $|J_z = -j\rangle$.

It can be seen from this figure that with the increasing of the effective atomic resonant frequency ω_0 in the standard two-axis twisting Hamiltonian $H_{\rm TAT}$, the maximal squeezing factor $\xi^2_{\rm M}$ increases, i.e., spin squeezing is reduced.

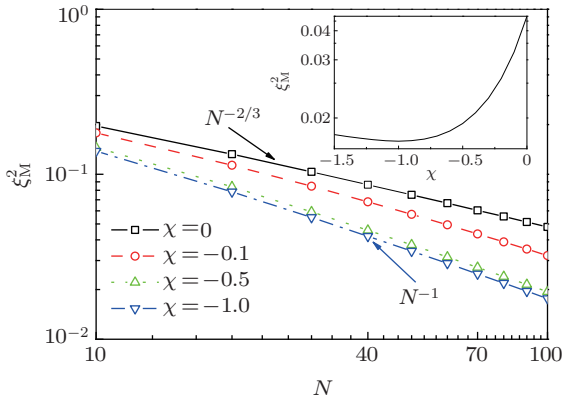


Fig. 3. (color online) Numerical plot of the maximal squeezing factors $\xi^2_{\rm M}$ as a function of the atomic number N for the different anisotropic parameters χ. Insert: numerical plot of the maximal squeezing factor $\xi^2_{\rm M}$ as a function of the anisotropic parameter χ, when the atomic number is chosen as $N=100$. In both subfigures, $q=1$ and the initial states are chosen as $|J_z=-j\rangle$.

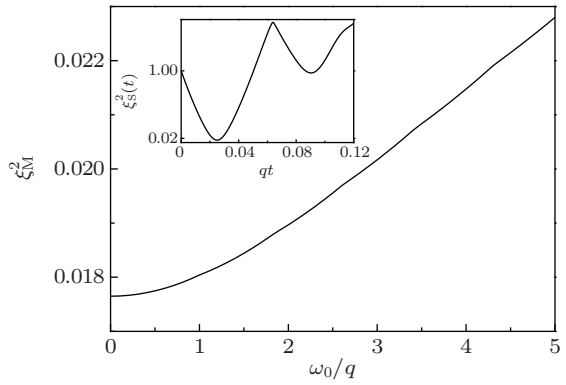


Fig. 4. (color online) Numerical plot of the maximal squeezing factor $\xi^2_{\rm M}$ as a function of the effective atomic resonant frequency ω_0. Insert: numerical plot of the time-dependent squeezing factor $\xi^2_{\rm S}(t)$, when $\omega_0/q=0.3$. In both subfigures, the initial states, the anisotropic parameter, and the atomic number are chosen as $|J_z=-j\rangle$, $\chi=-1$, and $N=100$, respectively.

According to the above discussion, we argue that when increasing the anisotropic parameter χ (from $\chi=-1$) or introducing the effective atomic resonant frequency ω_0 in the standard two-axis twisting Hamiltonian $H_{\rm TAT}$, the maximal squeezing factor $\xi^2_{\rm M}$ increases, i.e., spin squeezing is reduced. Surprisingly, when we control these two parameters simultaneously, spin squeezing can be enhanced greatly. To see this clearly, in Fig. 5 we numerically plot the maximal squeezing factors $\xi^2_{\rm M}$ of the generalized two-axis spin Hamiltonian (6), i.e., $H=q(J_x^2+\chi J_y^2)+\omega_0 J_z$, as a function of the effective atomic resonant frequency ω_0 for different anisotropic parameters χ, when the initial state is chosen as $|J_z=-j\rangle$. This figure shows that in the case of $\chi=-0.05$ or $\chi=-0.5$, when increasing the effective atomic resonant frequency ω_0, the maximal squeezing factor $\xi^2_{\rm M}$ first decreases greatly and then increases, i.e., spin squeezing is first enhanced greatly and then reduced. For the generalized one-axis twisting model $H_{\rm GOAT}=qJ_x^2+\omega_0 J_z$, the maximal squeezing factor $\xi^2_{\rm M}$ has a similar behavior (see green dashed-dotted line in Fig. 5),[59] but its magnitude cannot arrive at the order of our considered two-axis spin Hamiltonian (6), because these two Hamiltonians have different scalings with respect to the atomic number N. These results are of benefit for achieving the required spin squeezing in experiments.

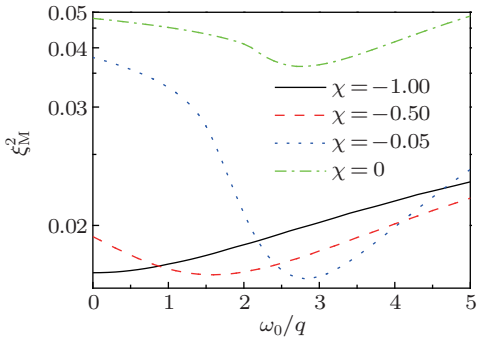


Fig. 5. (color online) Numerical plot of the maximal squeezing factors $\xi^2_{\rm M}$ as a function of the effective atomic resonant frequency ω_0 for the different anisotropic parameters χ. The initial state and the atomic number are chosen as $|J_z=-j\rangle$ and $N=100$, respectively.

5. The experimental feasibility

Finally, we address the experimental feasibility by considering ^{87}Rb atom, with the six levels depicted in Fig. 1. In this case, the decay rates of the atomic excited states and photons are about $\gamma/2\pi=6.0$ MHz and $\kappa/2\pi=1.3$ MHz (the ground states are stable and we do not need to consider the corresponding decays).[49,50] On the other hand, based on the transitions between the different levels, the atom–photon coupling strengths can reach $g_{s_1}/2\pi=20$ MHz and $g_{s_2}/2\pi=15$ MHz, respectively, both of which are much larger than the photon decay rate κ. As a consequence, the system is dominated by the Hamiltonian dynamics. When $\Omega_{s_1}/2\pi=20$ MHz and $\Delta_{s_1}/2\pi=100$ MHz, together with the above estimated parameter values, the adiabatic condition for deriving Eq. (A2) is reasonable, and moreover, we have $\lambda_1/2\pi=4$ MHz and $q/2\pi=0.8$ MHz for $\omega_{\rm A}/2\pi=-20$ MHz. This choice of the detuning $\omega_{\rm A}$ also satisfies the dispersive condition, which is a key condition to realize our generalized two-axis spin Hamiltonian (6). For the anisotropic parameter χ, it can be easily controlled by tuning both the detuning $\omega_{\rm B}$ and the Rabi frequency Ω_{s_2}.

When $N=100$ with above parameters, the numerical result shows that the shortest time for generating the maximal squeezing factor $\xi^2_{\rm M}$ is about $t_{\rm m}\simeq 25$ ns (see, for example, in the insert part of Fig. 4), which is shorter than the photon lifetime κ^{-1}. With the increase of the atomic number N, $t_{\rm m}$

becomes shorter and shorter, since $t_{\rm m} = 1/N^{0.8}$, as shown in Fig. 6. In the real experiments with $N = 10^4$ or 10^5,[49,50] $t_{\rm m} = 0.6$ ns or 0.1 ns. This indicates that the maximal spin squeezing can be created very quickly in experiments. Notice that for more rigorous consideration of the effect inducing the photon decay κ, we should use the method of quantum master equation. However, here we mainly take the first step to realize the two-axis twisting Hamiltonian and achieve spin squeezing (approaching the Heisenberg limit) in the two cavities.

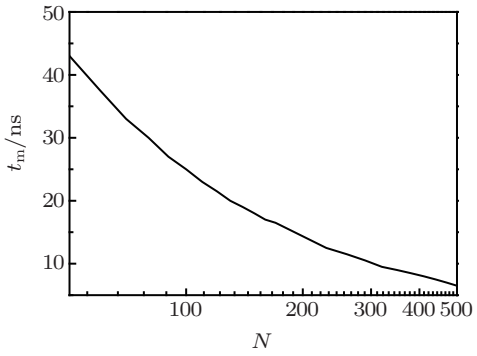


Fig. 6. Numerical plot of the shortest time $t_{\rm m}$ for generating the maximal squeezing factor as a function of the atomic number N. The initial state, the effective atomic resonant frequency, and the anisotropic parameter are chosen as $|J_z = -{\rm j}\rangle$, $\omega_0/q = 0.3$, and $\chi = -1$, respectively.

6. Conclusion

In summary, we have proposed an experimentally feasible system, in which an ensemble of ultracold six-level atoms interacts with two quantized cavity fields and two pairs of Raman lasers, to realize a generalized two-axis spin Hamiltonian $H = q(J_x^2 + \chi J_y^2) + \omega_0 J_z$. We have numerically calculated the experimentally measurable maximal squeezing factor and revealed that when $\omega_0 = 0$ and $\chi = -1$, the maximal squeezing factor $\xi_{\rm M}^2$ scales as N^{-1}. More importantly, we have found that by combining with the anisotropic parameter $\chi(> -1)$, the effective atomic resonant frequency ω_0 can enhance spin squeezing greatly. Our results are of benefit for achieving the required spin squeezing in experiments, and have a potential application in quantum information and quantum metrology.

Appendix A: Effective two-mode Dicke Hamiltonian

Substituting Eqs. (2)–(4) into Hamiltonian (1) yields

$$\begin{aligned}\widetilde{H} = {} & \Delta_{\rm a} a^\dagger a + \Delta_{\rm b} b^\dagger b + \sum_{j=1}^{N} \{\Delta_{r_1} |r_1\rangle_j\langle r_1|_j \\ & + \Delta_{r_2} |r_2\rangle_j\langle r_2|_j + \Delta_{s_1} |s_1\rangle_j\langle s_1|_j \\ & + \Delta_{s_2} |s_2\rangle_j\langle s_2|_j + \Delta_1 |1\rangle_j\langle 1|_j \\ & + \frac{1}{2}[\Omega_{s_1} |s_1\rangle_j\langle 1|_j {\rm e}^{{\rm i}\varphi_{s_1}} + \Omega_{s_2} |s_2\rangle_j\langle 1|_j {\rm e}^{{\rm i}\varphi_{s_2}} \\ & + \Omega_{r_1} |r_1\rangle_j\langle 0|_j {\rm e}^{{\rm i}\varphi_{r_1}} + \Omega_{r_2} |r_2\rangle_j\langle 0|_j {\rm e}^{{\rm i}\varphi_{r_2}} + {\rm H.c.}] \\ & + [g_{s_1} |s_1\rangle_j\langle 0|_j a + g_{r_1} |r_1\rangle_j\langle 1|_j a \\ & + g_{s_2} |s_2\rangle_j\langle 0|_j b + g_{r_2} |r_2\rangle_j\langle 1|_j b + {\rm H.c.}]\}, \end{aligned} \tag{A1}$$

where $\Delta_{\rm a} = \omega_{\rm a} - \widetilde{\omega_{\rm a}}$, $\Delta_{\rm b} = \omega_{\rm b} - \widetilde{\omega_{\rm b}}$, $\Delta_{s_1} = \omega_{s_1} - \widetilde{\omega_{s_1}}$, $\Delta_{s_2} = \omega_{s_2} - \widetilde{\omega_{s_2}}$, and $\Delta_1 = \omega_1 - \widetilde{\omega_1}$.

In the large detuning limit, i.e., $|\Delta_{r_{1,2},s_{1,2}}| \gg \{\Omega_{r_{1,2}}, \Omega_{s_{1,2}}, g_{r_{1,2}}, g_{s_{1,2}}, \gamma, \kappa\}$, all excited states can be eliminated adiabatically,[51] where γ and κ are the decay rates of the atomic excited states and photons, and an effective Hamiltonian is obtained by

$$\begin{aligned}\widetilde{H} = {} & \omega_{\rm A} a^\dagger a + \omega_{\rm B} b^\dagger b + \omega_0 J_z + \eta a^\dagger a J_z \\ & + [(\lambda_{r_1} a {\rm e}^{-{\rm i}\varphi_{r_1}} + \lambda_{r_2} b {\rm e}^{-{\rm i}\varphi_{r_2}}) J_- \\ & + (\lambda_{s_1} a {\rm e}^{-{\rm i}\varphi_{s_1}} + \lambda_{s_2} b {\rm e}^{-{\rm i}\varphi_{s_2}}) J_+ + {\rm H.c.}], \end{aligned} \tag{A2}$$

where $\eta = g_{r_1}^2/\Delta_{r_1} + g_{r_2}^2/\Delta_{r_2} - g_{s_1}^2/\Delta_{s_1} - g_{s_2}^2/\Delta_{s_2}$, $J_+ = \sum_{j=1}^{j=N} |1\rangle_j\langle 0|_j$, $J_- = \sum_{j=1}^{j=N} |0\rangle_j\langle 1|_j$, and $J_z = \sum_{j=1}^{j=N} (|1\rangle_j\langle 1|_j - |0\rangle_j\langle 0|_j)/2$ are the collective spin operators,

$$\omega_0 = \Delta_1 + \frac{1}{4}\left(\frac{\Omega_{s_1}^2}{\Delta_{s_1}} + \frac{\Omega_{s_2}^2}{\Delta_{s_2}} - \frac{\Omega_{r_1}^2}{\Delta_{r_1}} - \frac{\Omega_{r_2}^2}{\Delta_{r_2}}\right), \tag{A3}$$

$$\omega_{\rm A} = \Delta_{\rm a} + \frac{1}{2}\left(\frac{N g_{r_1}^2}{\Delta_{r1}} + \frac{N g_{s_1}^2}{\Delta_{s1}}\right), \tag{A4}$$

$$\omega_{\rm B} = \Delta_{\rm b} + \frac{1}{2}\left(\frac{N g_{r_2}^2}{\Delta_{r_2}} + \frac{N g_{s_2}^2}{\Delta_{s_2}}\right), \tag{A5}$$

are the effective atomic resonant frequency and the effective frequencies of two cavity modes a and b, respectively, and

$$\lambda_{r_i} = \frac{1}{2}\frac{g_{r_i}\Omega_{r_i}}{\Delta_{r_i}}, \lambda_{s_i} = \frac{1}{2}\frac{g_{s_i}\Omega_{s_i}}{\Delta_{s_i}} \quad (i = 1, 2) \tag{A6}$$

are the effective atom–photon coupling strengths.

When choosing $g_{r_i}^2/\Delta_{r_i} = g_{s_i}^2/\Delta_{s_i}$ and $\Omega_{r_i} g_{r_i}/\Delta_{r_i} = \Omega_{s_i} g_{s_i}/\Delta_{s_i}$, the Hamiltonian (A2) turns into

$$\begin{aligned}\widetilde{H} = {} & \omega_{\rm A} a^\dagger a + \omega_{\rm B} b^\dagger b + \omega_0 J_z \\ & + \left[\frac{\lambda_1}{2}(a J_+ {\rm e}^{-{\rm i}\varphi_{s_1}} + a J_- {\rm e}^{-{\rm i}\varphi_{r_1}}) \right. \\ & \left. + \frac{\lambda_2}{2}(b J_+ {\rm e}^{-{\rm i}\varphi_{s_2}} + b J_- {\rm e}^{-{\rm i}\varphi_{r_2}}) + {\rm H.c.}\right], \end{aligned} \tag{A7}$$

where the effective atom–photon coupling strengths become

$$\lambda_1 = \frac{\Omega_{s_1} g_{s_1}}{\Delta_{s_1}} = \frac{\Omega_{r_1} g_{r_1}}{\Delta_{r_1}}, \tag{A8}$$

$$\lambda_2 = \frac{\Omega_{s_2} g_{s_2}}{\Delta_{s_2}} = \frac{\Omega_{r_2} g_{r_2}}{\Delta_{r_2}}. \tag{A9}$$

The above consideration of the parameters has been used experimentally.[49,50] When applying a unitary transformation, $U = {\rm e}^{{\rm i}[(\varphi_{s_1} - \varphi_{r_1})J_z - (\varphi_{s_s} + \varphi_{r_2})b^\dagger b - (\varphi_{s_1} + \varphi_{r_1})a^\dagger a]/2}$, the Hamiltonian (A7) is rewritten as

$$\begin{aligned}\widetilde{H} = {} & \omega_{\rm A} a^\dagger a + \omega_{\rm B} b^\dagger b + \omega_0 J_z + \left[\frac{\lambda_1}{2}(a^\dagger + a)(J_+ + J_-) \right. \\ & \left. + \frac{\lambda_2}{2}(b + b^\dagger)(J_+ {\rm e}^{{\rm i}[(\varphi_{s_1} - \varphi_{s_2}) - (\varphi_{r_1} - \varphi_{r_2})]/2} \right. \end{aligned}$$

$$+J_{-}\,\mathrm{e}^{-\mathrm{i}[(\varphi_{s_1}-\varphi_{s_2})-(\varphi_{r_1}-\varphi_{r_2})]/2}\Big)\Big]. \tag{A10}$$

Notice that there exists a unitary invariant phase difference $[(\varphi_{s_1}-\varphi_{s_2})-(\varphi_{r_1}-\varphi_{r_2})]/2$, which can be chosen as $-\pi/2$ by sweeping the phases of Raman lasers. Thus, the Hamiltonian (A10) becomes the Hamiltonian (5).

References

[1] Kitagawa M and Ueda M 1993 *Phys. Rev. A* **47** 5138
[2] Ma J, Wang X, Sun C P, *et al*. 2011 *Phys. Rep.* **509** 89
[3] Robins N P, Altin P A, Debs J E, *et al*. 2013 *Phys. Rep.* **529** 265
[4] Duan L M, Sørensen A, Cirac J I, *et al*. 2000 *Phys. Rev. Lett.* **85** 5643
[5] Sørensen A, Duan L M, Cirac J I, *et al*. 2001 *Nature* **409** 63
[6] Santarelli G, Laurent P, Lemonde P, *et al*. 1999 *Phys. Rev. Lett.* **82** 4619
[7] Hammerer K, Sørensen A S and Polzik E S 2010 *Rev. Mod. Phys.* **82** 1041
[8] Helmerson K and You L 2001 *Phys. Rev. Lett.* **87** 170402
[9] Bouchoule I and Mølmer K 2002 *Phys. Rev. A* **65** 041803
[10] Zhang M, Helmerson K and You L 2003 *Phys. Rev. A* **68** 043622
[11] André A and Lukin M D 2002 *Phys. Rev. A* **65** 053819
[12] André A, Duan L M and Lukin M D 2002 *Phys. Rev. Lett.* **88** 243602
[13] Thomsen L K, Mancini S and Wiseman H M 2002 *J. Phys. B* **35** 4937
[14] Ng H T, Law C K and Leung P T 2003 *Phys. Rev. A* **68** 013604
[15] Cappellaro P and Lukin M D 2009 *Phys. Rev. A* **80** 032311
[16] Liu Y C, Xu Z F, Jin G R, *et al*. 2011 *Phys. Rev. Lett.* **107** 013601
[17] Shen C and Duan L M 2013 *Phys. Rev. A* **87** 051801
[18] Zhang J Y, Zhou X F, Guo G C, *et al*. 2014 *Phys. Rev. A* **90** 013604
[19] Huang W, Zhang Y L, Zou C L, *et al*. 2015 *Phys. Rev. A* **91** 043642
[20] Deb R N, Abdalla M Sebawe, Hassan S S and Nayak N 2006 *Phys. Rev. A* **73** 053817
[21] Nielsen A E B and Mølmer K 2008 *Phys. Rev. A* **77** 063811
[22] Schleier-Smith M H, Leroux I D and Vuletić V 2010 *Phys. Rev. A* **81** 021804
[23] Leroux I D, Schleier-Smith M H and Vuletić V 2010 *Phys. Rev. Lett.* **104** 073602
[24] Chen Z, Bohnet J G, Sankar S R, *et al*. 2011 *Phys. Rev. Lett.* **106** 133601
[25] Dalla Torre, Otterbach J, Demler E, Vuletić V, *et al*. 2013 *Phys. Rev. Lett.* **110** 120402
[26] Chen Z, Bohnet J G, Weiner J M, *et al*. 2014 *Phys. Rev. A* **89** 043837
[27] Yu L, Fan J, Zhu S, *et al*. 2014 *Phys. Rev. A* **89** 023838
[28] Auccaise R, Araujo-Ferreira A G, Sarthour R S, *et al*. 2015 *Phys. Rev. Lett.* **114** 043604
[29] Huang X Y, Xiang Y, Sun F X, *et al*. 2015 *Acta Phys. Sin.* **64** 160304 (in Chinese)
[30] Zhong W, Liu J, Ma J, *et al*. 2014 *Chin. Phys. B* **23** 060302
[31] Messina A, Maniscalco S and Napoli A 2003 *J. Mod. Phys.* **50** 1
[32] Mariantoni M, Deppe F, Marx A, Gross R, *et al*. 2008 *Phys. Rev. B* **78** 104508
[33] Mariantoni M, Wang H, Bialczak R C, *et al*. 2011 *Nat. Phys.* **7** 287
[34] Egger D J and Wilhelm F K 2013 *Phys. Rev. Lett.* **111** 163601
[35] Wickenbrock A, Hemmerling M, Robb G R M, *et al*. 2013 *Phys. Rev. A* **87** 043817
[36] Krimer D O, Liertzer M, Rotter S, *et al*. 2014 *Phys. Rev. A* **89** 033820
[37] McKay D C, Naik R, Reinhold P, *et al*. 2015 *Phys. Rev. Lett.* **114** 080501
[38] Larson J and Levin S 2009 *Phys. Rev. Lett.* **103** 013602
[39] Larson J 2010 *Phys. Rev. A* **81** 051803
[40] Gopalakrishnan S, Lev B L and Goldbart P M 2009 *Nat. Phys.* **5** 845
[41] Gopalakrishnan S, Lev B L and Goldbart P M 2010 *Phys. Rev. A* **82** 043612
[42] Gopalakrishnan S, Lev B L and Goldbart P M 2011 *Phys. Rev. Lett.* **107** 277201
[43] Strack P and Sachdev S 2011 *Phys. Rev. Lett.* **107** 277202
[44] Buchhold M, Strack P, Sachdev S, *et al*. 2013 *Phys. Rev. A* **87** 063622
[45] Andreanov A and Müller M 2012 *Phys. Rev. Lett.* **109** 177201
[46] Fan J, Yang Z, Zhang Y, *et al*. 2014 *Phys. Rev. A* **89** 023812
[47] Guzmán R, Retamal J C, Solano E, *et al*. 2006 *Phys. Rev. Lett.* **96** 010502
[48] Parkins A S, Solano E and Cirac J I 2006 *Phys. Rev. Lett.* **96** 053602
[49] Baumann K, Guerlin C, Brennecke F, *et al*. 2010 *Nature* **464** 1301
[50] Baden M P, Arnold K J, Grimsmo A L, *et al*. 2014 *Phys. Rev. Lett.* **113** 020408
[51] Dimer F, Estienne B, Parkins A S, *et al*. 2007 *Phys. Rev. A* **75** 013804
[52] Lipkin H J, Meshkov N and Glick N 1965 *Nucl. Phys. A* **62** 188
[53] Lipkin H J, Meshkov N and Glick N 1965 *Nucl. Phys. A* **62** 199
[54] Lipkin H J, Meshkov N and Glick N 1965 *Nucl. Phys. A* **62** 211
[55] Dusuel S and Vidal J 2004 *Phys. Rev. Lett.* **93** 237204
[56] Ribeiro P, Vidal J and Mosseri R 2007 *Phys. Rev. Lett.* **99** 050402
[57] Orús R, Dusuel S and Vidal J 2008 *Phys. Rev. Lett.* **101** 025701
[58] Chen G, Liang J Q and Jia S 2009 *Opt. Exp.* **17** 19682
[59] Law C K, Ng H T and Leung P T 2011 *Phys. Rev. A* **63** 055601
[60] Vidal J, Palacios G and Mosseri R 2004 *Phys. Rev. A* **69** 022107
[61] Vidal J, Mosseri R, and Dukelsky J 2004 *Phys. Rev. A* **69** 054101
[62] Morrison S and Parkins A S 2008 *Phys. Rev. Lett.* **100** 040403
[63] Chen G, Wang X, Liang J Q, *et al*. 2008 *Phys. Rev. A* **78** 023634
[64] Wineland D J, Bollinger J J, Itano W M, *et al*. 1992 *Phys. Rev. A* **46** R6797